Interactions of Thermophilic Microorganisms and Sulfur/Iron

A Dissertation Submitted to
the Graduate School of Life and Environmental Sciences,
the University of Tsukuba
in Partial Fulfillment of the Requirements
for the Degree of Doctor of Philosophy in Science
(Doctoral Program in Biological Sciences)

Kensuke IGARASHI

Abbreviations

EPS:	Exopolysaccharide
FE-SEM:	Field-emission scanning electron microscopy
SRB	Sulfate-reducing bacteria
TEM:	Transmission electron microscopy
XRD:	X-ray diffraction

Chapter 2 describes the reduction of hematite with sulfide derived from the reduction of S^0 by a thermophilic fermenter, *Thermosipho globiformans*, during syntrophy with *M. jannaschii* in a medium containing proteinaceous organics. S^0 is known to interrupt the H_2-mediated syntrophy between fermenter and methanogen by intercepting reducing equivalents from the fermenter, which otherwise reduce H^+ and produce H_2, resulting in the generation of sulfide. Hematite added to the S^0-intrrupted syntrophic system was converted to amorphous FeS by the reduction with the sulfide. The amorphous FeS formed a network of spiny structures due to the presence of proteinaceous organics. The network shielded S^0 in the sediment and recovered the syntrophy in the liquid milieu. Amorphous FeO(OH) instead of hematite also rescued the syntrophy by the same mechanism. These results suggest that the fermenter–methanogen syntrophy is possible also in the presence of S^0, if hematite or amorphous FeO(OH) is present. This implies that the oxidative force converting Fe(II) to Fe(III), such as oxygen molecules, may help methanogens survive at the border of anoxic and oxic environments.

interrupt the syntrophy. However, I revealed that addition of Fe(III) alleviated the interruption by S^0. Experimental evidence suggested that this phenomenon was explained by the stiffening of iron sulfide that shielded the S^0 in the sediment. From ecological point of view, I discussed the effect of Fe(III) on expanding the environmental niche of methanogens.

Chapter 2: Fe(III) oxides protect fermenter–methanogen syntrophy against interruption by elemental sulfur via stiffening of Fe(II) sulfides produced by sulfur respiration

Abstract

Thermosipho globiformans (rod-shaped thermophilic fermenter) and *Methanocaldococcus jannaschii* (coccal hyperthermophilic hydrogenotrophic methanogen) established H_2-mediated syntrophy at 68°C, forming exopolysaccharide-based aggregates. Electron microscopy showed that the syntrophic partners connected to each other directly or via intercellular bridges made from flagella, which facilitated transfer of H_2. Elemental sulfur (S^0) interrupted syntrophy; polysulfides abiotically formed from S^0 intercepted electrons that were otherwise transferred to H^+ to produce H_2, resulting in the generation of sulfide (sulfur respiration). However, Fe(III) oxides significantly reduced the interruption by S^0, accompanied by stiffening of Fe(II) sulfides produced by the reduction of Fe(III) oxides with the sulfur respiration-generated sulfide. Sea sand replacing Fe(III) oxides failed to generate stiffening or protect the syntrophy. Several experimental results indicated that the stiffening of Fe(II) sulfides shielded the liquid from S^0, resulting in methane production in the liquid. Field-emission scanning electron microscopy showed that the stiffened Fe(II) sulfides formed a network of spiny structures in which the microorganisms were buried. The individual fermenter rods likely produced Fe(II) sulfides on their surface and became local centers of a core of spiny structures, and the connection of these cores formed the network, which was macroscopically recognized as stiffening.

Introduction

Fermenter–methanogen syntrophy is an H_2/formate-mediated syntrophy in which H_2/formate is produced by fermenters and consumed by methanogens. In the H_2-mediated syntrophy, fermenters produce H_2 when intracellular substrates for fermentation have been exhausted; electrons are then transferred from reduced coenzymes to H^+, yielding H_2. However, this reaction is endergonic and tends to be reversed under physiological conditions, leading to the accumulation of reduced coenzymes, which results in growth inhibition of fermenters. Methanogens benefit from fermenter-produced H_2 as an energy source, resulting in the alleviation of H_2-inhibition of the fermenters (Stams and Plugge, 2009).

Bacterial as well as archaeal fermenters are involved in (hyper)thermophile syntrophy (Bonch-Osmolovskaya and Stetter, 1991; Ishii et al., 2005; Muralidharan et al., 1997; Schopf et al., 2008; Ver Eecke et al., 2012). Among them, syntrophic partnerships involving a bacterial fermenter and methanogen, such as *Thermotoga maritima* (Huber et al., 1986) with *Methanocaldococcus jannaschii* (Jones et al., 1983), or *Pelotomaculum thermopropionicum* (Imachi et al., 2002) with *Methanothermobacter thermautotrophicus* (Zeikus and Wolee, 1972), are better characterized(Ishii et al., 2005; Johnson et al., 2006; Johnson et al., 2005; Muralidharan et al., 1997; Shimoyama et al., 2009). The fermenters and methanogens approach each other through binding to fermenter-produced exopolysaccharides (EPSs) (Muralidharan et al., 1997) and by forming intercellular bridges (Ishii et al., 2005), which are expected to facilitate transfer of H_2.

Thermosipho globiformans (Kuwabara et al., 2011) is a thermophilic fermenter, belonging to the bacterial order Thermotogales (Huber and Stetter, 1992), recently shown to establish a syntrophy with *Mc. jannaschii* (Yamane et al., 2013). *T. globiformans* was

collected from a deep-sea hydrothermal vent using an *in situ* cultivation device that was designed to create interfaces between anoxic and oxic environments similar to those found in hydrothermal chimneys (Kuwabara et al., 2006). *T. globiformans* exhibited hematite-reducing activity, which was obvious in the presence of elemental sulfur (S^0) (Kuwabara et al., 2011).

H_2-mediated syntrophy is suggested in hydrothermal chimneys (Harmsen et al., 1997; Schrenk et al., 2003; Ver Eecke et al., 2012). However, the chimneys are well known to contain elemental sulfur (S^0) as well as metal sulfides (Jannasch, 1989; Noguchi et al., 2007; Watanabe and Kajimura, 1994). It is unknown whether the syntrophy is possible under such chemical environments; S^0 interrupts syntrophy (Muralidharan et al., 1997) because polysulfides, which are abiotically generated from S^0 and SH^- (Schauder and Kröger, 1993; Schauder and Müller, 1993; Teder, 1971), intercept electrons that are otherwise transferred to H^+, by a process known as sulfur respiration. However, metal sulfides at the surface of chimneys are oxidized with O_2 in seawater to generate metal oxides. Effects of metals oxides on the syntrophy in the presence of S^0 have not been studied.

In this study, the syntrophy of *T. globiformans* and *M. jannaschii* was characterized at first in the absence of both S^0 and Fe(III) oxides. Next, the effects of S^0 and Fe(III) oxides on the syntrophy were studied. The obtained results indicate that stiffening of Fe(II) sulfides, which are produced by the reduction of Fe(III) oxides with sulfur respiration-derived sulfide, shields the liquid from S^0, resulting in methane production in the liquid.

Materials & Methods

Strains and cultivation

T. globiformans MN14 was isolated in our laboratory (Kuwabara et al., 2011) and was deposited in the Japan Collection of Microorganisms (JCM) and Deutsche Sammlung von Mikroorganismen und Zellkulturen (DSMZ). *M. jannaschii* JAL-1 (Jones et al., 1983) and *T. maritima* MSB8 (Huber et al., 1986) were obtained from JCM.

Anaerobic cultivations were performed using 12 ml of medium in 68-ml serum bottles (Kuwabara et al., 2011). An anaerobic workstation was used for inoculation, in which the gas phase was N_2:H_2:CO_2 (80:10:10) (Kuwabara et al., 2005). *T. globiformans* was successively cultivated in Tc medium (pH 6.5) (Kuwabara et al., 2005) that contained the following per liter of H_2O: 25 g of NaCl, 0.33 g of KCl, 2.8 g of $MgCl_2 \cdot 6H_2O$, 3.4 g of $MgSO_4 \cdot 7H_2O$, 10 mg of NaBr, 0.3 g of K_2HPO_4, 0.25 g of NH_4Cl, 0.025 g of $FeSO_4 \cdot 7H_2O$, 10 ml each of trace mineral solution and vitamin solution (Balch et al., 1979), 3 g of Bacto-yeast extract, 3 g of Bacto-tryptone, 10 g of elemental sulfur (S^0), 0.5 g of $Na_2S \cdot 9H_2O$, and 1 mg of resazurin, under the headspace of workstation gas at 68°C for 16 h. *T. globiformans* was precultivated in Tc medium devoid of S^0 (Tc–S^0 medium) before syntrophic cocultivation. *M. jannaschii* was successively cultivated in JCM 232 medium under the headspace of H_2:CO_2 (80:20) at 80°C for 24 h. Cocultivation of *T. globiformans* and *M. jannaschii* was performed in Tc medium or Tc–S^0 medium, with or without addition of Fe(III) oxides equivalent to 60 mM Fe, at 68°C for 16 h, unless otherwise stated. Workstation gas was also used for the cocultivation because the same conditions were chosen for the hematite-reducing activity of *T. globiformans* (Kuwabara et al., 2011). In some experiments, the serum bottles were rotated during cocultivation using a hybridization incubator (HB-80; TAITEC, Koshigaya, Japan). As controls, *T. globiformans* or

M. jannaschii were monocultivated in Tc medium containing Fe(III) oxides at 68°C, under a headspace of workstation gas for 16 h and H_2:CO_2 (80:20) for 32 h, respectively.

T. maritima was successively cultivated in JCM 237 medium under the headspace of workstation gas at 80°C for 24 h. *T. maritima* and *M. jannaschii* were cocultivated at 68°C or 85°C under the same conditions as the monocultures.

Preparation of growth media containing Fe(III) oxides or sea sand

In this study, Fe(III) oxides were represented by hematite (purity >97%; Wako, Osaka, Japan) and amorphous FeO(OH). Hematite was washed once with distilled water and then suspended in distilled water to a concentration of 0.6 M. Amorphous FeO(OH) were prepared as described previously (Lovley and Phillips, 1986), washed 6 times with distilled water, and then suspended in distilled water to a concentration of 0.6 M. The Fe(III) oxide suspensions were autoclaved at 121°C for 20 min with a stir bar and were subsequently stored at room temperature. Aliquots of the suspensions were removed during stirring and were added to Tc medium to bring the calculated concentrations of Fe(III) to 60 mM, which yielded Tc+hematite medium and Tc+FeO(OH) medium, respectively.

The amounts of hematite and S^0 in the Tc+hematite medium were tripled, with layering of hematite on the S^0, which yielded Tc($3S^0$)+3hematite medium, which was used to clearly visualize S^0 remaining after cocultivation. As a control, the same packed volume of sea sand (particle size, 300–600 μm; Wako) was layered on the S^0 in place of Hematite, which yielded Tc($3S^0$)+sea sand medium. Before preparing the control medium, the sea sand was washed with Tc–S^0 medium by autoclaving and hand-operated centrifugation. The resulting pellet was resuspended in Tc–S^0 medium, autoclaved, and stored at room temperature.

Quantitative analyses

The cell density and levels of methane, sulfide, and Fe(II) were determined using 3 cultures unless otherwise stated, and duplicate measurements were averaged for each culture.

Cell density. Cells were enumerated by direct counting using bacteria counting chambers. Serum bottles were vigorously shaken to disperse cells from aggregates. An aliquot of each culture was transferred to a microcentrifuge tube with a syringe and mixed with a LIVE/DEAD® *Bac*Light™ Bacterial Viability Kit (LIVE/DEAD; Molecular Probes, Eugene, OR, USA) as described previously (Kuwabara et al., 2005), and 2 μl of the mixture was loaded onto the chamber by capillary action; large aggregates may have escaped the loading. Concentrated samples were diluted with sterile 2% (w/v) NaCl before mixing with LIVE/DEAD. The total number of cells were counted using an optical microscope (Eclipse E600; Nikon) equipped with blue light excitation (excitation, 450–490 nm; dichroic mirror, 505 nm; barrier filter, 520 nm), while the *M. jannaschii* cells were counted based on the F_{420} autofluorescence under violet light excitation (excitation, 380–420 nm; dichroic mirror, 430 nm; barrier filter, 450 nm). *T. globiformans* cells were calculated by subtracting the *M. jannaschii* cell number from the total cell number.

Methane. For the determination of methane, samples from the headspace gas were taken with a gas-tight syringe and subjected to gas chromatography (GC-14A; Shimadzu, Kyoto, Japan) operated at 50°C with a Porapak Q 80/100 column (4 m; GL Sciences, Tokyo, Japan) equipped with a 1-m pre-column of the same adsorbent (Nakamura et al., 1999). Helium was used as the carrier gas. Methane was detected using a thermal conductivity detector.

Sulfide and Fe(II). The amounts of sulfide and Fe(II) in sediments and supernatants were quantified by the methylene blue (Cline, 1969) and the ferrozine methods (Stookey, 1970) , respectively, as described in chapter 1 except that Fe(II) was extracted from the sediments by

mixing in 0.625 N HCl for 20 min at room temperature.

Conversion of soluble sulfide to gaseous H_2S might be considerable during the experimental operations, e.g., the centrifugation, at the pH after cocultivation (pH 6.3), at which the ratio of H_2S to HS^- at equilibrium is approximately 4:1 (Snoeyink and Jenkins, 1980). To estimate the removal of sulfide as gaseous H_2S, 50-µl aliquots were taken from a coculture to determine total sulfide, and the remainder was put into a 15-ml tube as described above. The 15-ml tube was not centrifuged but instead placed outside the workstation during the centrifugation. After returning the centrifuge tube into the workstation, 50-µl aliquots were taken from the suspension after shaking to determine gaseous H_2S-removed total sulfide. The amount of removed sulfide was estimated by subtracting the gaseous H_2S-removed total sulfide from the total sulfide. The sulfide removed from Tc+hematite medium and Tc medium were estimated to be 2% and 9% of the respective total sulfides, each the average of 2 cocultures. The amounts of sulfide are shown without correction in the figures.

Electron microscopy

For field-emission scanning electron microscopy (FE-SEM), cultivation was performed in the presence of a glass SEM plate (diameter, 8.5 mm). The plate was carefully taken out of the medium and processed as described previously (Kuwabara and Igarashi, 2012). Mixtures of monocultures of *T. globiformans* and *M. jannaschii* grown in Tc–S^0 medium, and the sediments that had not stiffened in the Tc+hematite medium were placed on a glass SEM plate, which had been coated with 0.1% (w/v) poly-L-lysine. After standing for 30 min at room temperature, these specimens were fixed and processed for observation as described previously (Kuwabara and Igarashi, 2012).

For whole mount transmission electron microscopy (TEM), cultivation was performed

with carbon-coated (Näther et al., 2006) or formvar-coated gold grids placed at the bottom of serum bottles. After cultivation, the grids were taken out of the serum bottles using tweezers and immediately fixed with 2% glutaraldehyde buffered with 0.2 M sodium cacodylate (pH 7.2) for 30 min, washed with the same buffer for 10 min, and negatively stained with 2% uranyl acetate for 1 min. The specimens were observed with a TEM (JEM1010; JEOL, Tokyo, Japan) at an acceleration voltage of 80 kV.

Results

Syntrophy of *T. globiformans* and *M. jannaschii* in Tc–S^0 medium

The syntrophy of *T. globiformans* and *M. jannaschii* was first characterized in Tc–S^0 medium. The microbes established syntrophy within 24 h at 68°C, 17°C below the optimal growth temperature of the methanogen, even when both organisms were inoculated at only 1×10^5 cells/ml (Fig. 9). Monocultures of the methanogen showed no apparent growth, suggesting that the essential energy source in the coculture was the H_2 produced by the fermenter. When the initial headspace was replaced from the workstation gas to 100% N_2, similar growth levels were attained after 16 h (Table 2).

Aggregate formation

Tiny black pellets were observed in the cocultures from the early stage of the mid-exponential phase; some pellets floated in the medium and other pellets adhered to the glassware (Fig. 10a). Similar pellets were observed even when the cocultures were rotated using a hybridization incubator (Fig. 10b). The pellets contained aggregates of syntrophic partners and EPS (Fig. 11), as observed using phase-contrast and fluorescence microscopy with acridine orange and Fluorescent Brightener 28 (Ishii et al., 2005; Johnson et al., 2006; Johnson et al., 2005; Muralidharan et al., 1997; Shimoyama et al., 2009). No apparent differences were observed among the pellets in different locations, regardless of the rotation of the serum bottle. The aggregates were preserved even in the stationary phase (Fig. 10).

Intercellular bridge formation and direct connection between syntrophic partners

FE-SEM studies. To observe the fine structure of the aggregates, a glass SEM plate

was placed in the culture medium. FE-SEM of the pellets on the plate showed intercellular bridges as well as bridges connecting the cells and the glass substrate (Fig. 12a, b). Most bridges were narrow and straight (Fig. 12a; *arrowhead*), but wide and tapered bridges were also observed (Fig. 12b; *arrowhead*). The widths of the narrow-and-straight bridges ranged 50–100 nm, depending on the assembly (Fig. 12a, b; *diamond*). When monocultures of *T. globiformans* and *M. jannaschii* in Tc–S^0 medium were mixed at room temperature and subjected to FE-SEM analysis, no intercellular bridges were observed, indicating that the bridges observed in the cocultures were not an artifact of fixation (Dohnalkova et al., 2011). The narrow-and-straight bridges were also found in cocultures of *T. maritima* and *M. jannaschii* at 68°C, but not at 85°C (Muralidharan et al., 1997).

Some *T. globiformans* and *M. jannaschii* cells made direct contact during cocultivation (Fig. 12a). Similar contact was observed using optical microscopy as well as FE-SEM in the mixtures of the monocultures, suggesting that the syntrophic partners have an affinity for one another. The rotation of the cocultures or replacement of the headspace with 100% N_2 did not affect these structural features.

TEM studies. Whole mount TEM of the pellets that sedimented on carbon-coated gold grids (Näther et al., 2006) revealed that the bridges had formed from the tufts of the flagella (Fig. 12c). Because *M. jannaschii* has flagella (Jones et al., 1983), and like most *Thermosipho* species, no flagella have been observed for *T. globiformans* (Kuwabara et al., 2011), the methanogen likely provided the bridges. When the carbon-coated gold grids were replaced by formvar-coated grids, the flagella were observed with better resolution (Fig. 12d). Interestingly, the TEM images showed that some bridge-forming flagella were combined at the tips, on the fermenters (Fig. 12c). This finding suggests that the methanogen captures the fermenter using the flagella. Alternatively, the *T. globiformans* flagella could be generated in

response to the syntrophy (see Discussion).

The TEM images also showed a structure directly connecting the cells of the syntrophic partners, penetrating the Thermotogales-specific large periplasm (Fig. 12e). The presence of this internal structure confirms that the contact between the syntrophic partners observed using FE-SEM (Fig. 12a) was not an artifact of fixation. This structure likely serves to transfer fermenter-produced H_2 directly to the methanogen.

Some wide-and-tapered bridges appeared to protrude from the rods (Fig. 12b; *star*) and could be compositionally distinct from the narrow-and-straight bridges or a result of fixation of the loosened tips from the *M. jannaschii* flagella. *T. globiformans* formed intercellular bridges made from nanotubes of toga (Fig. 12f) in monocultures in Tc–S^0 medium (Kuwabara and Igarashi, 2012), but whole mount TEM did not show such intercellular bridges between syntrophic partners. The origin of the wide-and-tapered bridges remains to be elucidated.

Effects of S^0 and hematite on syntrophy

Addition of S^0 at 312 mM (10 g/l) to Tc–S^0 medium, which yielded Tc medium, enhanced the growth of *T. globiformans* but interrupted syntrophy, as observed with no growth of methanogen, producing approximately 4 mM soluble sulfide due to sulfur respiration (Fig. 13). However, when 30 mM hematite was added to Tc medium, which yielded Tc+hematite medium, the methanogen grew in the presence of S^0 (Fig. 13). Accompanying the recovery of syntrophy, the sediment turned from reddish brown to black and stiffened (Fig. 14b, c); the sediment layers were not broken when the serum bottles were tilted. Addition of hematite to Tc–S^0 medium, which yielded Tc–S^0+hematite medium, did not enhance syntrophy (Fig. 13), suggesting that the syntrophy-rescuing ability of hematite was related to the presence of S^0.

Stiffening of Fe(II) sulfides protects syntrophy

Sulfide and Fe(II) were significant in the sediment after cocultivation in Tc+hematite medium (Fig. 13), suggesting that the stiffened black substance was Fe(II) complexed with sulfides [Fe(II) sulfides]. When the serum bottles were rotated during the cocultivation to physically prevent stiffening, the interruption of syntrophy by S^0 was reproduced (Fig. 13). Because the rotation did not affect syntrophy in the absence of S^0 (Fig. 13), the interruption must be caused by the absence of stiffening. To investigate the causal relationship between the stiffening and methane production, the cell density, levels of methane, sulfide, and Fe(II), as well as the stiffening of the sediment, were measured every 4 h during cocultivation in Tc+hematite medium. Solid sulfide and Fe(II) increased up to 12 h from the start of cocultivation; stiffening was detected from 8 h (Fig. 14c), while methane production was first detected from 12 h (Fig. 15). The fact that stiffening preceded methane production suggested that the stiffening caused methane production, likely by shielding the liquid from S^0.

The methane production could be due to exhaust of S^0, although the white appearance in the bottom view of Fig. 14c suggested residual S^0. Therefore, the amounts of S^0 and hematite in Tc+hematite medium were tripled, with the hematite layered on top of the S^0, which yielded Tc($3S^0$)+3hematite medium. Cocultivation in Tc($3S^0$)+3hematite medium produced methane amounting to 60% of that found in Tc+hematite medium (Table 3); however, S^0 clearly remained under the stiffened Fe(II) sulfides (Fig. 14d). Next, I tested whether syntrophy occurs when materials other than Fe(III) oxides cover the S^0. Hematite in Tc($3S^0$)+3hematite medium was replaced by the same packed volume of sea sand, which yielded Tc($3S^0$)+sea sand medium. Cocultivation in Tc($3S^0$)+sea sand medium gave no stiffening of the sediment (Fig. 14e), with no methane production (Table 3). These results suggest that stiffening is essential for the

protection of syntrophy.

Effects of the hematite-to-S^0 ratio on methane production

To investigate the effects of the hematite-to-S^0 ratio on methane production, *T. globiformans* and *M. jannaschii* were cocultivated in Tc medium containing increasing concentrations of hematite. Up to an hematite-to-S^0 molar ratio of 0.0025, the amount of soluble sulfide was high, stiffening of the sediment did not occur, and no methane was detected during the cocultivation (Fig. 16). However, at a molar ratio of 0.005, the sediment stiffened, solid sulfide increased, and methane was detected. Methane significantly increased at a ratio of 0.01, and above 0.01, methane gradually increased along with an increase in solid Fe(II). These findings suggest that there is a threshold hematite-to-S^0 ratio in the range of 0.0025–0.01 for syntrophy protection, and the shielding was more or less leaky but became more effective with the increase in solid Fe(II).

Biological process involved in the reduction of hematite with sulfide

M. jannaschii is known to utilize S^0 as an electron acceptor (Stetter and Gaag, 1983). To assess the contribution of the methanogen to the reduction of hematite, each microorganism was monocultivated in Tc+hematite medium. *T. globiformans* produced stiffened Fe(II) sulfides after 16 h of cultivation (Fig. 14f), while *M. jannaschii* did not produce stiffened Fe(II) sulfides, even after 32 h of cultivation, under the headspace of H_2:CO_2 (80:20) (Fig. 14g). This finding suggests that the methanogen contributed little to the reduction of hematite during cocultivation.

The reduction of hematite in Tc+hematite medium involves 2 processes: sulfide production by sulfur respiration of the fermenter and hematite reduction by the sulfide. The

latter process might be abiotic (Dos Santos Afonso and Stumm, 1992). To assess the significance of abiotic hematite reduction, Tc+hematite medium was supplemented with 40 mM Na_2S (pH 7.0), 10-fold higher concentration than that produced upon cocultivation in Tc medium (Fig. 13), and the resulting medium was incubated without inoculum. After incubation, the soluble sulfide remained high, and the production of either soluble or solid Fe(II) was insignificant (Fig. 13). This finding suggests that hematite was not easily reduced with abiotic sulfide and that a biological process was involved in the reduction of hematite.

Stiffened Fe(II) sulfides show a network of spiny structures

FE-SEM of the sediment from cocultures in Tc+hematite medium showed spiny structures (Fig. 17a, b). The microorganisms were partially or fully buried in the network of the spiny structures; it was challenging to recognize the fully buried microorganisms, but characteristic bridges protruding from a core of spiny structures suggested the presence of microorganisms (Fig. 17b, *oval*). The spiny structures were never observed in the sediments from cocultures in Tc–S^0+hematite medium (Fig. 17c), which showed the reddish brown color of hematite (Fig. 14a), suggesting that the spiny structures were related to Fe(II) sulfides.

The network of spiny structures was also produced by *T. globiformans* monocultures (Fig. 17d), but not by *M. jannaschii* monocultures, under the headspace of H_2:CO_2 (80:20) (Fig. 17e), consistent with the identification of spiny structures as Fe(II) sulfides. Abiotic incubation in Tc+hematite medium supplemented with 40 mM Na_2S (pH 7.0) produced a smaller amount of Fe(II) sulfides (Fig. 13), but without stiffening (Fig. 14h). FE-SEM of the sediments did not show the network of spiny structures, but instead showed tiny spines on the surface of hematite (Fig. 17f), suggesting that these spines were products of abiotic reduction of hematite with sulfide. Continued formation of tiny spines by the fermenter would construct the network of

spiny structures.

Effects of amorphous Fe(III) oxyhydroxide on syntrophy

To study the effects of Fe(III) oxides without a crystal structure, some experiments were repeated by replacing hematite with FeO(OH). Similar results were obtained (Figs. 18 and 19), although some differences were observed, such as lower growth levels of both species, higher amounts of cultivation- and incubation-produced Fe(II) sulfides (Fig. 18), and no abiotic production of tiny spines (Fig. 19e), probably related to the absence of a crystal structure of FeO(OH). When the cocultivation was performed in Tc medium containing 15 mM FeO(OH) for 32 h, the partial pressure of methane reached 1.2 ± 0.04 kPa (mean ± SD, n = 3). These results indicate that FeO(OH) also have the ability to protect syntrophy against interruption by S^0, although the methane production was decreased due to the toxicity of FeO(OH) to both microorganisms (Fig. 18).

Discussion

T. globiformans and *M. jannaschii* established syntrophy at 68°C, 17°C below the optimum growth temperature of the methanogen, 85°C (Jones et al., 1983). Direct contact between the syntrophic partner cells and the formation of intercellular bridges as well as EPS-based aggregates in the stationary phase compensated the drooping effects of suboptimal growth temperature for the methanogen. In the syntrophy of *T. maritima* and *M. jannaschii*, intercellular bridges did not form at 85°C (Muralidharan et al., 1997), and the aggregates decreased in the stationary phase due to the decrease in EPS formation (Johnson et al., 2006). However, I found intercellular bridges also in their syntrophy at 68°C. Given that similar bridges were also formed in other syntrophic pairs (Ishii et al., 2005; Schopf et al., 2008), the bridge formation could be a common feature of (hyper)thermophilic syntrophic partners.

The intercellular bridges between *T. globiformans* and *M. jannaschii* were likely to be made from the flagella of the methanogen (Fig. 12). Nevertheless, the possibility remains that the syntrophy enhanced the synthesis of flagella in *T. globiformans* ; although the *T. globiformans* genome has not been studied, the genomes of *Thermosipho africanus* TCF52B (Nesbø et al., 2009) and *Thermosipho melanesiensis* BI429 (Zhaxybayeva et al., 2009) have been shown to contain genes involved in flagellar synthesis. In contrast, the bridges between *P. furiosus* and *M. kandleri* were suggested to be the flagella of the archaeal fermenter (Schopf et al., 2008). Furthermore, the intercellular bridges between *P. thermopropionicum* and *M. thermautotrophicus* are made from the bacterial flagella (Ishii et al., 2005). These bridges must have a common function, bringing fermenters and methanogen closer. However, the origin-specific functions of the flagella, if any, must be different. The flagellar tip protein FliD of *P. thermopropionicum* transfers the signal that enhances the metabolism of *M.*

thermautotrophicus (Shimoyama et al., 2009). In contrast, the origin-specific functions of the intercellular bridges made of archaeal flagella, of either fermenters or methanogens, remain to be investigated.

This study revealed that Fe(III) oxides protect fermenter–methanogen syntrophy against interruption by S^0 through Fe(II) sulfide formation. Interestingly, sulfide, the product of sulfur respiration that interrupts syntrophy, is involved in the recovery of syntrophy. The stiffening appears to be essential for syntrophy protection, preventing the mixing of sedimented S^0 with the liquid. The finding that the same packed volume of sea sand gave neither stiffening (Fig. 14e) nor recovery of methane production (Table 3) suggests that the gaps between individual particles of sea sand (particle size, 300–600 μm) are sufficiently wide for the S^0 to mix with the liquid.

The effects of the hematite-to-S^0 molar ratio on methane production (Fig. 16) indicate that there is a threshold ratio for the observation of methane production in the range of 0.0025 to 0.01. I speculate that this threshold is related to the area of the cross section of the serum bottles, which should be shielded with Fe(II) sulfides for the methanogen to produce methane. In the range where the ratio is smaller than the threshold, the area of the cross section may be too wide to be shielded with existing Fe(II) sulfides. In contrast, in the range where the ratio is larger than the threshold, the Fe(II) sulfides should cover the cross section, and the layer would thicken with the increase in the availability of solid Fe(II), thereby more effectively restricting the permeation of S^0 and resulting in an hematite-to-S^0 ratio-dependent increase in methane production (Fig. 16).

Both hematite and FeO(OH) supported fermenter–methanogen syntrophy in the presence of S^0. However, FeO(OH) showed toxicity, especially to the methanogen, both in the presence and absence of S^0 (Fig. 18). This toxicity may be related to soluble Fe(II) produced by

the reduction of FeO(OH) (Dos Santos Afonso and Stumm, 1992; Pyzik and Sommer, 1981). The concentrations of soluble Fe(II) were calculated to 160 μM and 2.0 mM after cocultivation in Tc–S^0+hematite medium (Fig. 13) and Tc–S^0+FeO(OH) medium (Fig. 18), respectively, while the Fe(II) concentration in Tc–S^0 medium was approximately 90 μM (Kuwabara et al., 2005). The Fe(II) concentration in JCM 232 medium for *M. jannaschii* was lower than that in Tc medium. A soluble Fe(II) concentration that is 20-fold greater than the optimal is likely to be detrimental to both microorganisms.

Protection of methane production by Fe(III) oxides was accompanied by the stiffening of Fe(II) sulfides that formed a network of spiny structures (Figs. 17a, 17b, and 19a). Rods buried in the spiny structures suggested that sulfur respiration-derived sulfide reduced Fe(III) oxides on the bacterial surface. The individual fermenter rods likely functioned as local centers producing a core of spiny structures, and the connection of these cores formed the network, which was macroscopically recognized as stiffening of Fe(II) sulfides.

Hydrothermal chimneys contain S^0 and metal sulfides (Jannasch, 1989; Noguchi et al., 2007; Watanabe and Kajimura, 1994), but metal oxides such as Fe(III) oxides are generated at the surface by the oxidation with O_2 in seawater (Francheteau et al., 1979). The finding that methanogens were more abundant in outer fragments of chimneys than inner fragments (Harmsen et al., 1997; Schrenk et al., 2003) appears consistent with the result in this study that Fe(III) oxides rescue the syntrophy in the presence of S^0.

It may be argued that both microorganisms and S^0 come from the interior of the chimneys; if so, how does the shielding occur by the reduction of Fe(III) oxides located at the surface of chimneys? Recently, I found that cocultivation in Tc medium containing dacite pumice produced methane amounting to 10% of that found in Tc–S^0 medium containing dacite pumice (unpublished). This finding suggests that the microporous structures of dacite pumice

provided the microenvironment, into which S^0 particles hardly entered. It is expected that microporous structures of chimneys (Tivey and Singh, 1997) function similarly for syntrophy.

It is of note that (semi)conductive iron oxides (hematite and magnetite) facilitate syntrophy of *Geobacter* species and methanogens, as an electron sink for the metabolism of bacteria (Kato et al., 2012). Although the exact mechanism of how the iron oxide electron sinks facilitates syntrophy remains unknown, the syntrophy-promoting effects of iron oxides are similar to those revealed in the present study. Nevertheless, it remains to be established whether O_2 in oxic environments helps methanogens survive in anoxic environments thorough production of solid Fe(III) oxides at the border.

References

Anthony, J.W., and R.A. Bideaux. 1990. Greigite. *In* Handbook of Mineralogy. I (Elements, Sulfides, Sulfosalts). K.W. Bladh and M.C. Nichols, editors. Mineralogical Society of America, Chantilly, VA.

Balch, W.E., G.E. Fox, L.J. Magrum, C.R. Woese, and R.S. Wolfe. 1979. Methanogens: reevaluation of a unique biological group. *Microbiol. Rev.* 43:260-296.

Bandyopadhyay, S., K. Chandramouli, and M.K. Johnson. 2008. Iron-sulphur cluster biosynthesis. *Biochem. Soc. Trans.* 36:1112-1119.

Bauer, E., K.L. Man, A. Pavlovska, A. Locatelli, T.O. Mentes, M.A. Nino, and M.S. Altman. 2014. Fe_3S_4 (greigite) formation by vapor-solid reaction. *J. Mater. Chem. A*. 2:1903-1913.

Beinert, H., R.H. Holm, and E. Münck. 1997. Iron-sulfur clusters: nature's modular, multipurpose structures. *Science*. 277:653-659.

Berner, R.A. 1964. Iron sulfides formed from aqueous solution at low temperatures and atmospheric pressure. *J. Geol.* 72:293 - 306.

Bertel, D., J. Peck, T.J. Quick, and J.M. Senko. 2012. Iron transformations induced by an acid-tolerant *Desulfosporosinus* species. *Appl. Environ. Microbiol.* 78:81-88.

Bonch-Osmolovskaya, E.A., and K.O. Stetter. 1991. Interspecies hydrogen transfer in cocultures of thermophilic *Archaea*. *Syst. Appl. Microbiol.* 14:205-208.

Braterman, P.S., A.G. Cairns-Smith, and R.W. Sloper. 1983. Photo-oxidation of hydrated Fe^{2+}-significance for banded iron formations. *Nature*. 303:163-164.

Brock, T.D., and K. O'Dea. 1977. Amorphous ferrous sulfide as a reducing agent for culture of anaerobes. *Appl. Environ. Microbiol.* 33:254-256.

Bult, C.J., O. White, G.J. Olsen, L. Zhou, R.D. Fleischmann, G.G. Sutton, J.A. Blake, L.M. FitzGerald, R.A. Clayton, J.D. Gocayne, A.R. Kerlavage, B.A. Dougherty, J.-F. Tomb, M.D. Adams, C.I. Reich, R. Overbeek, E.F. Kirkness, K.G. Weinstock, J.M. Merrick, A. Glodek, J.L. Scott, N.S.M. Geoghagen, J.F. Weidman, J.L. Fuhrmann, D. Nguyen, T.R. Utterback, J.M. Kelley, J.D. Peterson, P.W. Sadow, M.C. Hanna, M.D. Cotton, K.M. Roberts, M.A. Hurst, B.P. Kaine, M. Borodovsky, H.-P. Klenk, C.M. Fraser, H.O. Smith, C.R. Woese, and J.C. Venter. 1996. Complete genome sequence of the methanogenic archaeon, *Methanococcus jannaschii*. *Science*. 273:1058-1073.

Cao, F., W. Hu, L. Zhou, W. Shi, S. Song, Y. Lei, S. Wang, and H. Zhang. 2009. 3D Fe_3S_4 flower-like microspheres: high-yield synthesis via a biomolecule-assisted solution approach, their electrical, magnetic and electrochemical hydrogen storage properties. *Dalton Trans.*:9246-9252.

Chang, Y.-S., S. Savitha, S. Sadhasivam, C.-K. Hsu, and F.-H. Lin. 2011. Fabrication, characterization, and application of greigite nanoparticles for cancer hyperthermia. *J. Colloid Interface Sci.* 363:314-319.

Chen, J.-S., and L.E. Mortenson. 1977. Inhibition of methylene blue formation during determination of the acid-labile sulfide of iron-sulfur protein samples containing dithionite. *Anal. Biochem.* 79:157-165.

Cline, J.D. 1969. Spectrophotometric determination of hydrogen sulfide in natural waters. *Limnol. Oceanogr.* 14:454-458.

Cornwell, J.C., and J.W. Morse. 1987. The characterization of iron sulfide minerals in anoxic marine sediments. *Mar. Chem.* 22:193-206.

Dilg, A., G. Mincione, K. Achterhold, O. Iakovleva, M. Mentler, C. Luchinat, I. Bertini, and F. Parak. 1999. Simultaneous interpretation of Mossbauer, EPR and 57Fe ENDOR spectra

of the [Fe_4S_4] cluster in the high-potential iron protein I from *Ectothiorhodospira halophila*. *J. Biol. Inorg. Chem.* 4:727-741.

Dohnalkova, A.C., M.J. Marshall, B.W. Arey, K.H. Williams, E.C. Buck, and J.K. Fredrickson. 2011. Imaging hydrated microbial extracellular polymers: comparative analysis by electron microscopy. *Appl. Environ. Microbiol.* 77:1254-1262.

Dos Santos Afonso, M., and W. Stumm. 1992. Reductive dissolution of iron(III) (hydr)oxides by hydrogen sulfide. *Langmuir*. 8:1671-1675.

Drobner, E., H. Huber, G. Wächtershäuser, D. Rose, and K.O. Stetter. 1990. Pyrite formation linked with hydrogen evolution under anaerobic conditions. *Nature*. 346:742-744.

Feng, M., Y. Lu, Y. Yang, M. Zhang, Y.-J. Xu, H.-L. Gao, L. Dong, W.-P. Xu, and S.-H. Yu. 2013. Bioinspired greigite magnetic nanocrystals: chemical synthesis and biomedicine applications. *Sci. Rep.* 3:1-6.

Flynn, T.M., E.J. O'Loughlin, B. Mishra, T.J. DiChristina, and K.M. Kemner. 2014. Sulfur-mediated electron shuttling during bacterial iron reduction. *Science*. 344:1039-1042.

Francheteau, J., H.D. Needham, P. Choukroune, T. Juteau, M. Séguret, R.D. Ballard, P.J. Fox, W. Normark, A. Carranza, D. Cordoba, J. Guerrero, C. Rangin, H. Bougault, P. Cambon, and R. Hekinian. 1979. Massive deep-sea sulphide ore deposits discovered on the East Pacific Rise. *Nature*. 277:523-528.

Gramp, J.P., J.M. Bigham, F.S. Jones, and O.H. Tuovinen. 2010. Formation of Fe-sulfides in cultures of sulfate-reducing bacteria. *J. Hazard. Mater.* 175:1062-1067.

Harmsen, H., D. Prieur, and C. Jeanthon. 1997. Distribution of microorganisms in deep-sea hydrothermal vent chimneys investigated by whole-cell hybridization and enrichment culture of thermophilic subpopulations. *Appl. Environ. Microbiol.* 63:2876-2883.

Hazen, R.M. 2013. Paleomineralogy of the Hadean eon: a preliminary species list. *Am. J. Sci.* 313:807-843.

Huber, R., T.A. Langworthy, H. König, M. Thomm, C.R. Woese, U.B. Sleytr, and K.O. Stetter. 1986. *Thermotoga maritima* sp. nov. represents a new genus of unique extremely thermophilic eubacteria growing up to 90°C. *Arch. Microbiol.* 144:324-333.

Huber, R., and K.O. Stetter. 1992. The order Thermotogales. *In* The Prokaryotes. A. Balows, H.G. Trüper, M. Dworkin, W. Harder, and K.H. Schleifer, editors. Springer, New York. 3809-3815.

Hunger, S., and L.G. Benning. 2007. Greigite: a true intermediate on the polysulfide pathway to pyrite. *Geochem. Trans.* 8:1.

Imachi, H., Y. Sekiguchi, Y. Kamagata, S. Hanada, A. Ohashi, and H. Harada. 2002. *Pelotomaculum thermopropionicum* gen. nov., sp. nov., an anaerobic, thermophilic, syntrophic propionate-oxidizing bacterium. *Int. J. Syst. Evol. Microbiol.* 52:1729-1735.

Ishii, S., T. Kosaka, K. Hori, Y. Hotta, and K. Watanabe. 2005. Coaggregation facilitates interspecies hydrogen transfer between *Pelotomaculum thermopropionicum* and *Methanothermobacter thermautotrophicus*. *Appl. Environ. Microbiol.* 71:7838-7845.

Janecky, D.R., and W.E. Seyfried Jr. 1986. Hydrothermal serpentinization of peridotite within the oceanic crust: Experimental investigations of mineralogy and major element chemistry. *Geochim. Cosmochim. Acta*. 50:1357-1378.

Jannasch, H.W. 1989. Sulphur emission and transformations at deep sea hydrothermal vents. *In* Evolution of the global biogeochemical sulphur cycle. P. Brimblecombe and A.Y. Lein, editors. John Wiley & Sons Ltd, New York. 181-190.

Johnson, M.R., S.B. Conners, C.I. Montero, C.J. Chou, K.R. Shockley, and R.M. Kelly. 2006. The *Thermotoga maritima* phenotype is impacted by syntrophic interaction with

Methanococcus jannaschii in hyperthermophilic coculture. *Appl. Environ. Microbiol.* 72:811-818.

Johnson, M.R., C.I. Montero, S.B. Conners, K.R. Shockley, S.L. Bridger, and R.M. Kelly. 2005. Population density-dependent regulation of exopolysaccharide formation in the hyperthermophilic bacterium *Thermotoga maritima*. *Mol. Microbiol.* 55:664-674.

Jones, W.J., J.A. Leigh, F. Mayer, C.R. Woese, and R.S. Wolfe. 1983. *Methanococcus jannaschii* sp. nov., an extremely thermophilic methanogen from a submarine hydrothermal vent. *Arch. Microbiol.* 136:254-261.

Kato, S., K. Hashimoto, and K. Watanabe. 2012. Methanogenesis facilitated by electric syntrophy via (semi)conductive iron-oxide minerals. *Environ. Microbiol.* 14:1646-1654.

Klimmek, O., Wiebke Dietrich, Felician Dancea, Yi-Jan Lin, Stefania Pfeiffer, Frank Löhr, Heinz Rüterjans, Roland Gross, Jörg Simon, and A. Kröger. 2004. Respiration in Archaea and Bacteria. Springer, New York. 217-232 pp.

Kuwabara, T., and K. Igarashi. 2012. Microscopic studies on *Thermosipho globiformans* implicate a role of the large periplasm of Thermotogales. *Extremophiles*. 16:863-870.

Kuwabara, T., A. Kawasaki, I. Uda, and A. Sugai. 2011. *Thermosipho globiformans* sp. nov., an anaerobic thermophilic bacterium that transforms into multicellular spheroids with a defect in peptidoglycan formation. *Int. J. Syst. Evol. Microbiol.* 61:1622-1627.

Kuwabara, T., M. Minaba, Y. Iwayama, I. Inouye, M. Nakashima, K. Marumo, A. Maruyama, A. Sugai, T. Itoh, J. Ishibashi, T. Urabe, and M. Kamekura. 2005. *Thermococcus coalescens* sp. nov., a cell-fusing hyperthermophilic archaeon from Suiyo Seamount. *Int. J. Syst. Evol. Microbiol.* 55:2507-2514.

Kuwabara, T., M. Minaba, H. Saida, T. Urabe, and M. Kamekura. 2006. A novel in situ cultivation device for isolation of thermophilic anaerobes of deep-sea hydrothermal

vents. *Biosystem Studies*. 9:218-227.

Lefèvre, C.T., N. Menguy, F. Abreu, U. Lins, M.t.l. Pósfai, T. Prozorov, D. Pignol, R.B. Frankel, and D.A. Bazylinski. 2011. A cultured greigite-producing magnetotactic bacterium in a novel group of sulfate-reducing bacteria. *Science*. 334:1720-1723.

Liu, Y., M. Sieprawska-Lupa, W.B. Whitman, and R.H. White. 2010. Cysteine is not the sulfur source for iron-sulfur cluster and methionine biosynthesis in the methanogenic archaeon *Methanococcus maripaludis*. *J. Biol. Chem.* 285:31923-31929.

Lovley, D.R., D.E. Holmes, and K.P. Nevin. 2004. Dissimilatory Fe(III) and Mn(IV) reduction advances in microbial physiology. Academic Press. 219-286.

Lovley, D.R., and E.J.P. Phillips. 1986. Organic matter mineralization with reduction of ferric iron in anaerobic sediments. *Appl. Environ. Microbiol.* 51:683-689.

Macleod, G., C. McKeown, A.J. Hall, and M.J. Russell. 1994. Hydrothermal and oceanic pH conditions of possible relevance to the origin of life. *Origins Life Evol. Biosphere*. 24:19-41.

Muralidharan, V., K.D. Rinker, I.S. Hirsh, E.J. Bouwer, and R.M. Kelly. 1997. Hydrogen transfer between methanogens and fermentative heterotrophs in hyoperthermophilic cocultures. *Biotechnol. Bioeng.* 56:268-278.

Näther, D.J., R. Rachel, G. Wanner, and R. Wirth. 2006. Flagella of *Pyrococcus furiosus*: multifunctional organelles, made for swimming, adhesion to various surfaces, and cell-cell contacts. *J. Bacteriol.* 188:6915-6923.

Nakamura, T., Y. Nojiri, M. Utsumi, T. Nozawa, and A. Otsuki. 1999. Methane emission to the atmosphere and cycling in a shallow eutrophic lake. *Arch. Hydrobiol.* 144:383-407.

Nesbø, C.L., E. Bapteste, B. Curtis, H. Dahle, P. Lopez, D. Macleod, M. Dlutek, S. Bowman, O. Zhaxybayeva, N.-K. Birkeland, and W.F. Doolittle. 2009. The genome of *Thermosipho*

africanus TCF52B: lateral genetic connections to the *Firmicutes* and *Archaea*. *J. Bacteriol.* 191:1974-1978.

Noguchi, T., T. Oomori, A. Tanahara, N. Taira, J. Takada, and H. Taira. 2007. Chemical composition of hydrothermal ores from Mid-Okinawa Trough and Suiyo Seamount determined by neutron activation analysis. *Geochem. J.* 41:141-148.

Paolella, A., C. George, M. Povia, Y. Zhang, R. Krahne, M. Gich, A. Genovese, A. Falqui, M. Longobardi, P. Guardia, T. Pellegrino, and L. Manna. 2011. Charge transport and electrochemical properties of colloidal greigite (Fe_3S_4) nanoplatelets. *Chem. Mater.* 23:3762-3768.

Pyzik, A.J., and S.E. Sommer. 1981. Sedimentary iron monosulfides: kinetics and mechanism of formation. *Geochim. Cosmochim. Acta*. 45:687-698.

Rabus, R., T.A. Hansen, and F. Widdel. 2013. The Prokaryotes. Springer, New York.

Rickard, D., and G.W. Luther III. 2007. Chemistry of iron sulfides. *Chem. Rev.* 107:514-562.

Russell, M.J., and A.J. Hall. 1997. The emergence of life from iron monosulphide bubbles at a submarine hydrothermal redox and pH front. *J. Geol. Soc.(London)*. 154:377-402.

Russell, M.J., and A.J. Hall. 2006. The onset and early evolution of life. *Geol. Soc. Am.* 198:1-32.

Russell, M.J., and W. Martin. 2004. The rocky roots of the acetyl-CoA pathway. *Trends Biochem. Sci.* 29:358-363.

Schauder, R., and A. Kröger. 1993. Bacterial sulphur respiration. *Arch. Microbiol.* 159:491-497.

Schauder, R., and E. Müller. 1993. Polysulfide as a possible substrate for sulfur-reducing bacteria. *Arch. Microbiol.* 160:377-382.

Schopf, S., G. Wanner, R. Rachel, and R. Wirth. 2008. An archaeal bi-species biofilm formed by *Pyrococcus furiosus* and *Methanopyrus kandleri*. *Arch. Microbiol.* 190:371-377.

Schrenk, M.O., D.S. Kelley, J.R. Delaney, and J.A. Baross. 2003. Incidence and diversity of microorganisms within the walls of an active deep-sea sulfide chimney. *Appl. Environ. Microbiol.* 69:3580-3592.

Shimoyama, T., S. Kato, S. Ishii, and K. Watanabe. 2009. Flagellum mediates symbiosis. *Science*. 323:1574.

Skinner, B.J., R.C. Erd, and F.S. Grimaldi. 1964. Greigite, the thio-spinel of iron; a new mineral. *Am. Mineralogist*. 49:543-555.

Snoeyink, V.L., and D. Jenkins. 1980. Water Chemistry. John Wiley & Sons, New York,.

Stams, A.J.M., and C.M. Plugge. 2009. Electron transfer in syntrophic communities of anaerobic bacteria and archaea. *Nat. Rev. Microbiol.* 7:568-577.

Stetter, K.O. 1996. Hyperthermophilic procaryotes. *FEMS Microbiol. Rev.* 18:149-158.

Stetter, K.O., and G. Gaag. 1983. Reduction of molecular sulphur by methanogenic bacteria. *Nature*. 305:309-311.

Stookey, L.L. 1970. Ferrozine-A new spectrophotometric reagent for iron. *Anal. Chem.* 42:779-781.

Teder, A. 1971. The equilibrium between elementary sulfur and aqueous polysulfide solutions. *Acta Chem. Scand.* 25:1722-1728.

Tivey, M.K., and S. Singh. 1997. Nondestructive imaging of fragile sea-floor vent deposit samples. *Geology*. 25:931-934.

Ver Eecke, H.C., D.A. Butterfield, J.A. Huber, M.D. Lilley, E.J. Olson, K.K. Roe, L.J. Evans, A.Y. Merkel, H.V. Cantin, and J.F. Holden. 2012. Hydrogen-limited growth of hyperthermophilic methanogens at deep-sea hydrothermal vents. *Proc. Natl. Acad. Sci. USA*. 109:13674-13679.

Wächtershäuser, G.u.n. 1992. Groundworks for an evolutionary biochemistry: the iron-sulphur

world. *Prog. Biophys. Molec. Biol.* 58:85-201.

Wada, H. 1977. The synthesis of greigite from a polysulfide solution at about 100°C. *Bull. Chem. Soc. Japan*. 50:2615-2617.

Watanabe, K., and T. Kajimura. 1994. The hydrothermal mineralization at Suiyo Seamount, in the central part of the Izu-Ogasawara Arc. *Resource Geol.* 44:133-140.

Yamane, K., S. Matsuyama, K. Igarashi, T. Utsumi, Y. Shiraiwa, and T. Kuwabara. 2013. Anaerobic co-culture of microalgae with *Thermosipho globiformans* and *Methanocaldococcus jannaschii* at 68°C enhances generation of *n*-alkane-rich biofuels after pyrolysis. *Appl. Environ. Microbiol.* 79:924-930.

Zeikus, J.G., and R.S. Wolee. 1972. *Methanobacterium thermoautotrophicus* sp. n., an anaerobic, autotrophic, extreme thermophile. *J. Bacteriol.* 109:707-713.

Zhaxybayeva, O., K.S. Swithers, P. Lapierre, G.P. Fournier, D.M. Bickhart, R.T. DeBoy, K.E. Nelson, C.L. Nesbø, W.F. Doolittle, J.P. Gogarten, and K.M. Noll. 2009. On the chimeric nature, thermophilic origin, and phylogenetic placement of the Thermotogales. *Proc. Natl. Acad. Sci. U.S.A.* 106:5865-5870.

Table 2. **Comparison of the workstation gas, N_2:H_2:CO_2 (80:10:10), and 100% N_2 in the headspace of syntrophic cocultures.** *T. globiformans* and *M. jannaschii* were cocultivated in Tc–S^0 medium for 16 h under the designated headspace. Values are expressed as the mean ± SD (n = 3).

	Cell density		Methane
Headspace	*T. globiformans*	*M. jannaschii*	
	(10^8 cells/ml)	(10^7 cells/ml)	(kPa)
Workstation gas	4.4 ± 0.9	1.9 ± 0.2	3.0 ± 0.6
100% N_2	4.0 ± 0.3	1.9 ± 0.3	3.2 ± 0.4

Table 3. **Cell densities and methane production in Tc+hematite medium, Tc(3S^0)+3hematite medium, and Tc(3S^0)+sea sand medium.** *T. globiformans* and *M. jannaschii* were cocultivated in the designated media for 16 h. Values are expressed as the mean ± SD (n = 3).

Culture	Cell density		Methane
medium	*T. globiformans*	*M. jannaschii*	
	(10^8 cells/ml)	(10^7 cells/ml)	(kPa)
Tc+hematite	3.6 ± 0.6	1.5 ± 0.5	1.2 ± 0.2
Tc(3S^0)+3 hematite	3.7 ± 0.6	1.0 ± 0.2	0.7 ± 0.1
Tc(3S^0)+sea sand	3.5 ± 0.2	0.0 ± 0.0	0

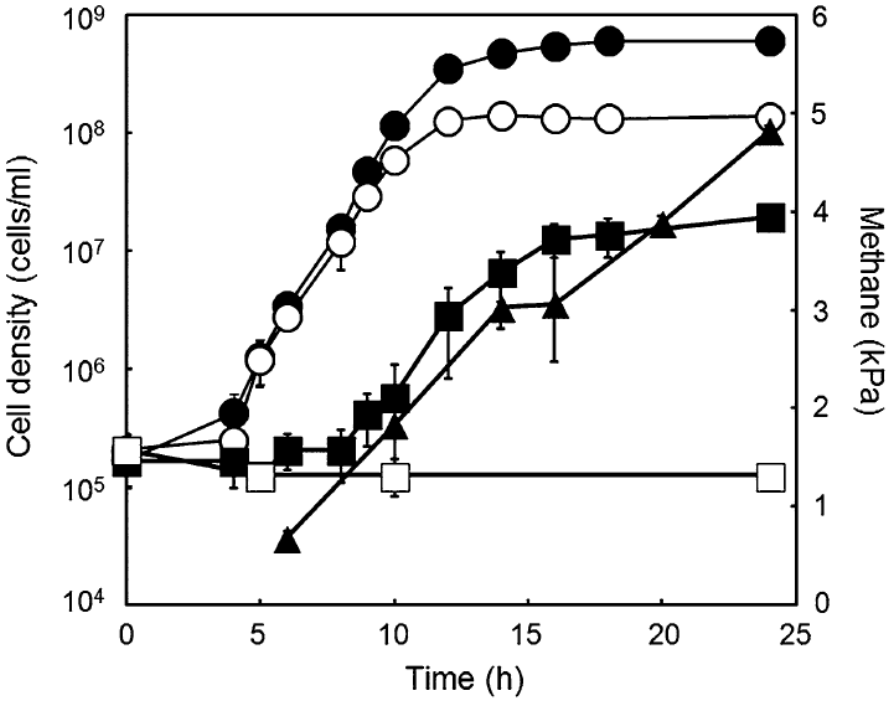

Fig. 9. Growth curves and methane production on syntrophy.

T. globiformans and *M. jannaschii* were cocultivated in Tc–S^0 medium at 68°C under the headspace of N_2:H_2:CO_2 (80:10:10) (n = 3). Cell densities of *T. globiformans* (circles) and *M. jannaschii* (squares) in the cocultures (closed symbols) are shown with those in the respective monocultures (open symbols). Methane in the headspace (closed triangles) was determined using cultures separate from those for the measurement of the growth curves. When the standard deviations are too small, the error bars are hidden by symbols.

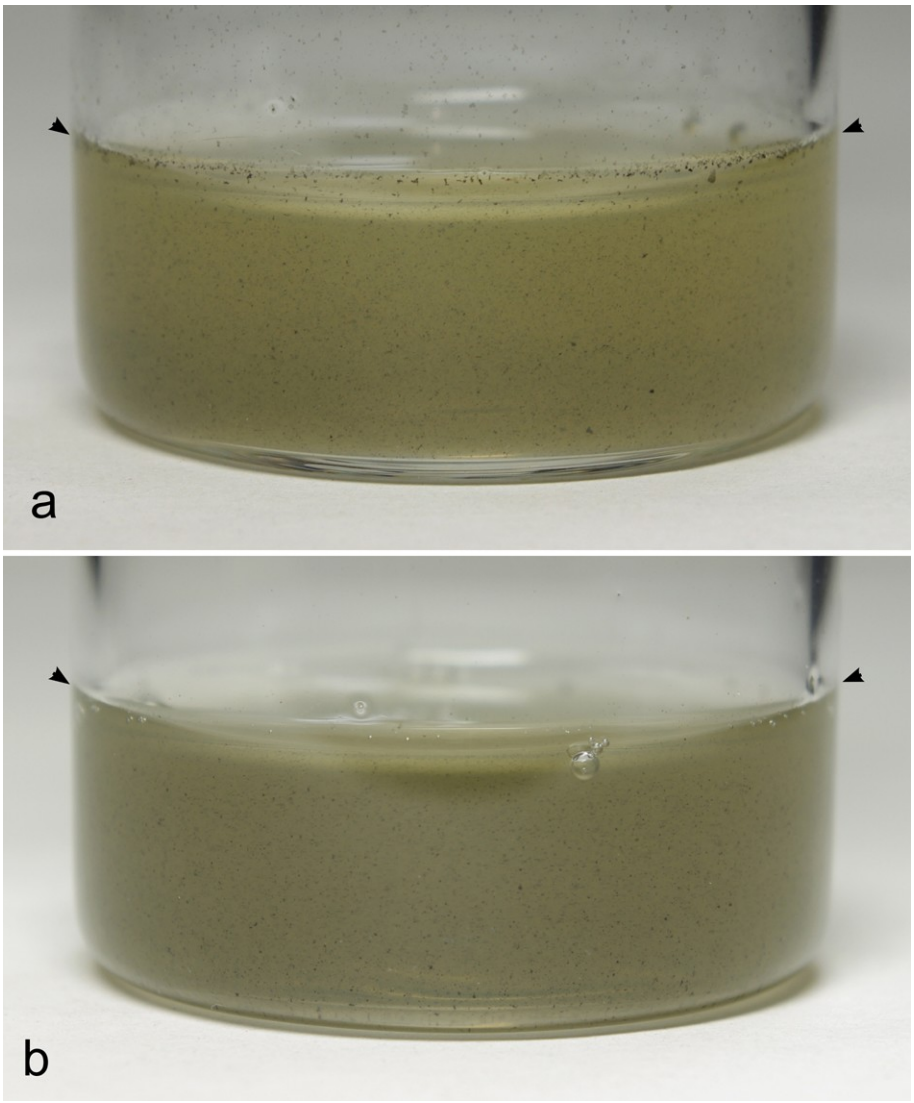

Fig. 10. Tiny black pellets generated in Tc–S^0 medium.

T. globiformans and *M. jannaschii* were cocultivated for 16 h. (**a**) Standing culture. (**b**) Rotated culture. Floating tiny black pellets are visible in the 2 cultures, with the difference of pellets adhering to the meniscus line (*arrowheads*) in the standing culture.

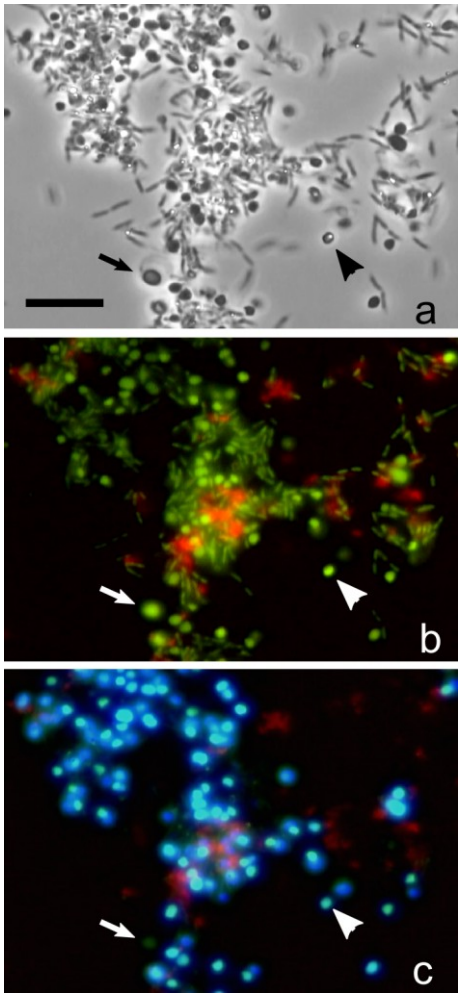

Fig. 11. Optical microscopy of tiny black pellets generated in Tc–S^0 medium.

(**a**) Phase-contrast microscopy image. (**b** and **c**) Fluorescence microscopy images with blue and violet light excitations. *T. globiformans* and *M. jannaschii* were cocultured in Tc–S^0 medium. A 20-µl aliquot of culture containing tiny black pellets was supplemented with 20 µl of 100 µg/ml Fluorescent Brightener 28 and 1 µl of 0.05% (w/v) acridine orange (in 10 mM sodium phosphate, pH 7.0). Images were obtained from snapshots of a color movie captured as described previously (Kuwabara and Igarashi, 2012). All cells were stained green by blue light excitation (panel **b**), and *Mc. jannaschii* cells were distinguished by their F_{420} autofluorescence by violet light excitation (panel **c**). EPS was stained red/orange. Spheroids of *T. globiformans* (*arrow*) were distinguished from *Mc. jannaschii* cells (*arrowhead*) by the large periplasm

observed in the phase-contrast microscope image and the significant decrease in fluorescence after violet light excitation. Bar = 10 μm.

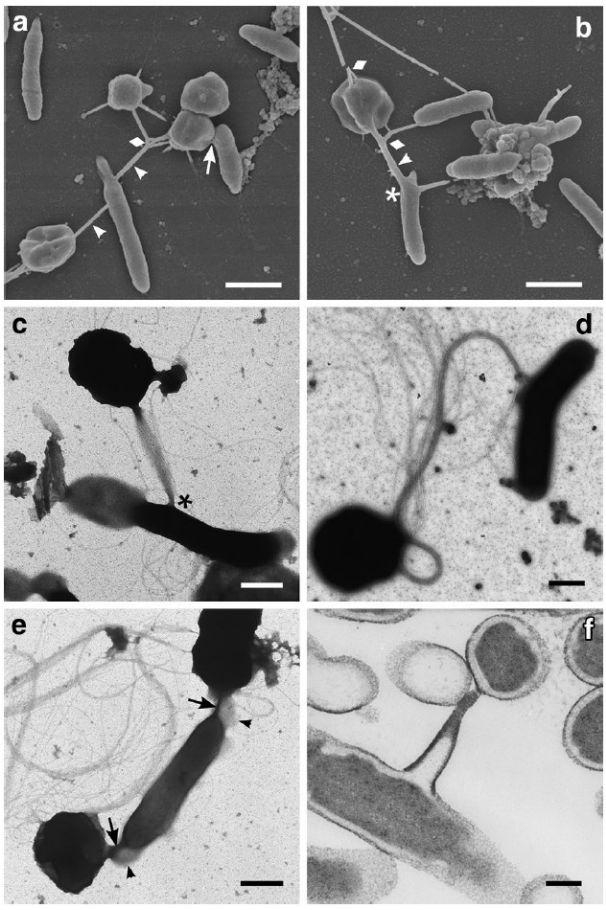

Fig. 12. FE-SEM and TEM images of intercellular bridges between and direct connection of syntrophic partners.

Cocultivation was performed in Tc–S^0 medium with a glass SEM plate (for FE-SEM) or with a gold grid (for TEM). (**a** and **b**) FE-SEM images showing narrow-and-straight and wide-and-tapered bridges (*white arrowheads*). The *diamond* shows assembly of bridges, the *white arrow* shows attachment of syntrophic partners, and the *white star* indicates the bridge portion that appears to be protruding from the rod. (**c** and **d**) Whole mount TEM images showing the flagellar structures of the intercellular bridges, taken with carbon-coated and formvar-coated gold grids. The *black asterisk* shows the combining of flagella at the surface of a rod. (**e**) Whole mount TEM image showing structures connecting cells of syntrophic partners (*black arrows*), which appear to penetrate the Thermotogales-specific large periplasm at the

ends of a rod (*black arrowheads*). (**f**) Thin section of monocultured *T. globiformans*, observed as described previously (Kuwabara and Igarashi, 2012), which shows a nanotube made from toga attaching to another rod that is situated perpendicular to the plane. Bars = 1 μm (**a**, **b**), 500 nm (**c**–**e**), and 200 nm (**f**).

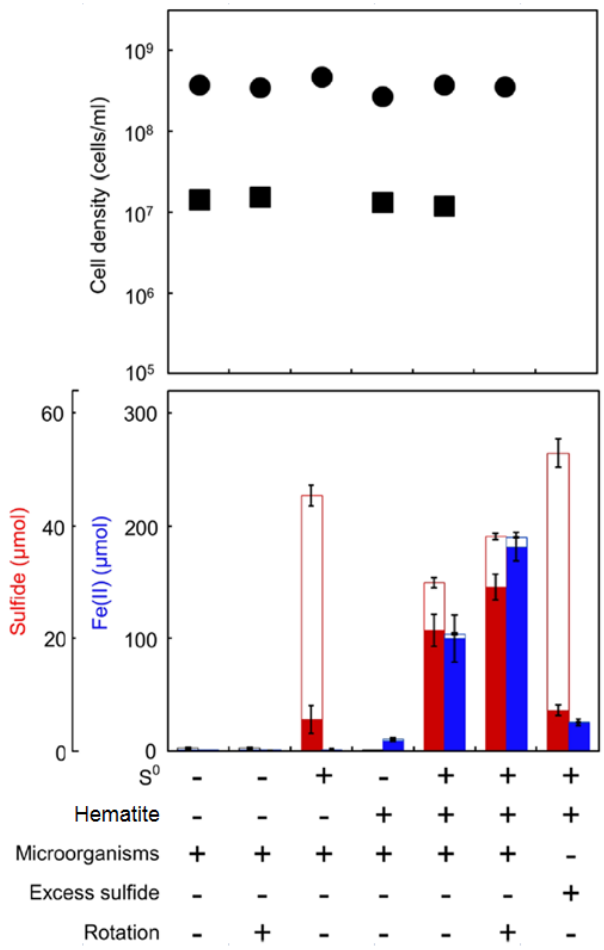

Fig. 13. Reduction of S^0 and hematite by cocultivation or incubation.

Cocultivation was performed under the conditions shown in the table below the lower graph. Cell densities of *T. globiformans* (circles) and *M. jannaschii* (squares) are plotted in the upper graph, while sulfide and Fe(II) are shown in the lower graph, in which the open and closed red bars indicate soluble and solid sulfides, respectively, and the open and solid blue bars indicate soluble and solid Fe(II), respectively. When the standard deviations are too small, the error bars are hidden by symbols.

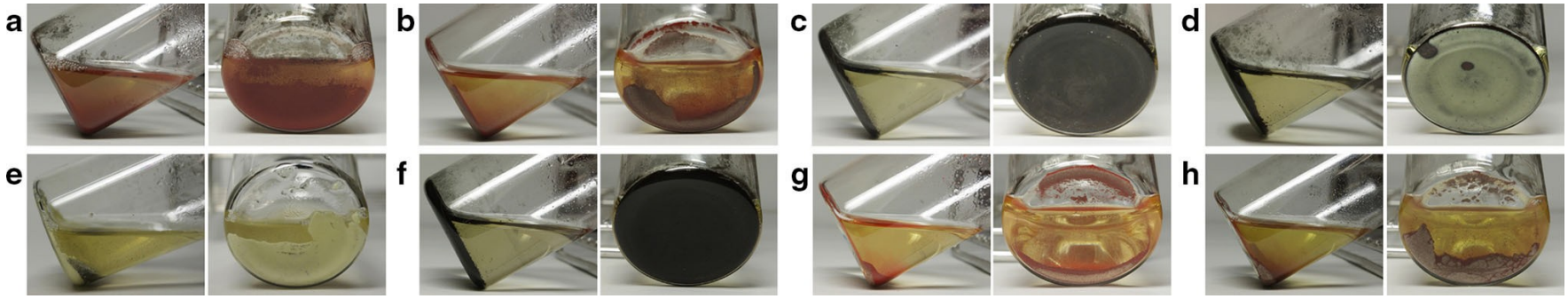

Fig. 14. Photos showing the color and stiffening of the sediments in hematite-containing media.

(**a**–**e**) Cocultivation was performed in (**a**) Tc–S^0+hematite medium, (**b**, **c**) Tc+hematite medium for 4 h and 8 h, (the images after 16 h of cocultivation are very similar to those after 8 h of cocultivation), (**d**) Tc($3S^0$)+3hematite medium, and (**e**) Tc($3S^0$)+sea sand medium. (**f**) *T. globiformans* was monocultivated in Tc+hematite medium. (**g**) *M. jannaschii* was monocultivated in Tc+hematite medium. (**h**) Tc+hematite medium supplemented with 40 mM Na_2S (pH 7.0) was abiotically incubated at 68°C for 16 h, similar to the cocultivation. Photos show the side and bottom views of the serum bottles.

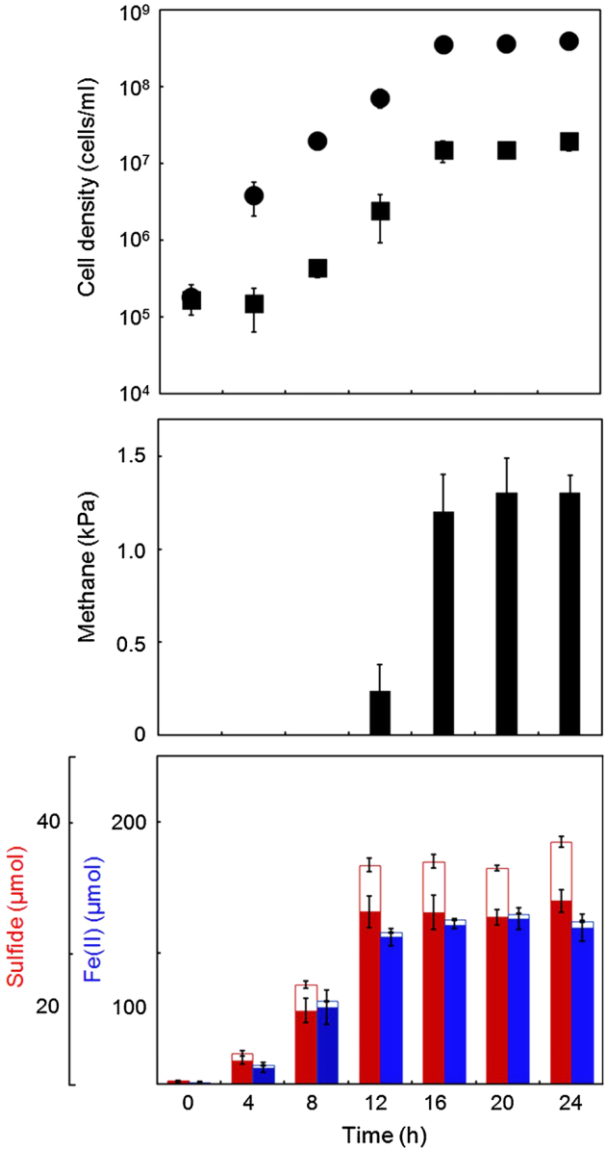

Fig. 15. Growth curve and the time course for the production of methane, sulfide, and Fe(II) during cocultivation in Tc+hematite medium.

Cell densities of *T. globiformans* (circles) and *M. jannaschii* (squares) are plotted in the upper graph, the methane partial pressure is shown in the middle graph, and the sulfide and Fe(II) levels are shown in the bottom graph in the same format as in Fig. 13. When the standard deviations are too small, the error bars are hidden by symbols.

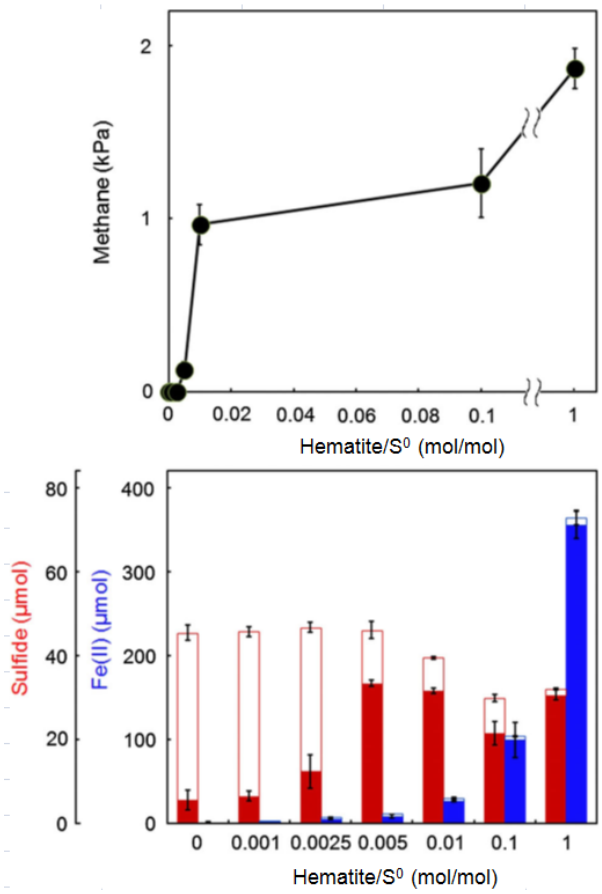

Fig. 16. Effects of the hematite-to-S^0 ratio in cocultivation media on the production of methane, sulfide, and Fe(II).

Cocultivation was performed in Tc medium containing different concentrations of hematite. The methane partial pressures are plotted in the upper graph, and the sulfide and Fe(II) produced at each ratio are shown in the lower graph, in the same format as in Fig. 13. The hematite-to-S^0 ratio of 0.1 corresponds to Tc+hematite medium. When the standard deviations are too small, the error bars are hidden by symbols.

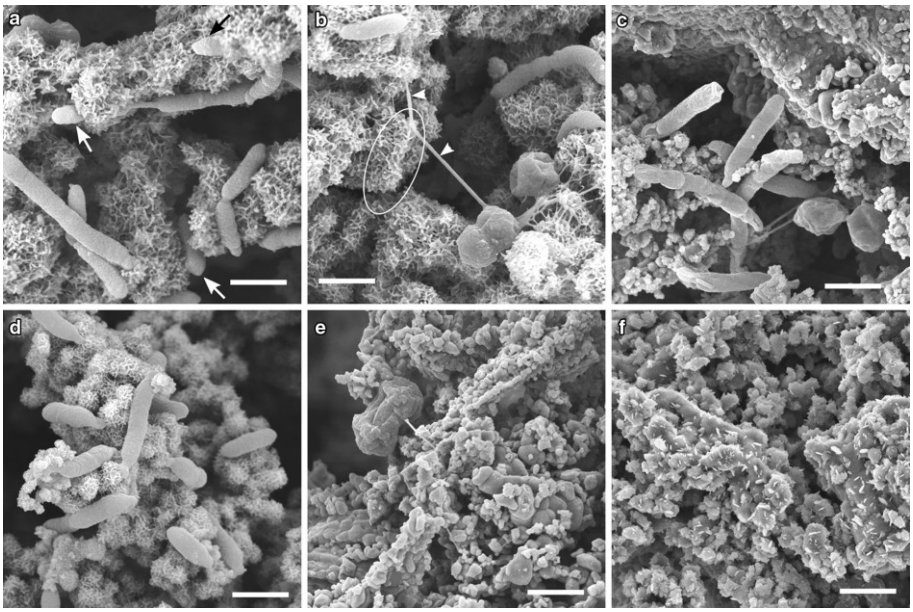

Fig. 17. FE-SEM images of the sediments of hematite-containing media.

(**a**, **b**) Tc+hematite medium after cocultivation. *Arrows* in panel A indicate rods partially buried in the network of spiny structures. *Arrowheads* and *oval* in panel B indicate narrow-and-straight bridges and a possible rod enclosed by spiny structures, respectively, which is suggested by the presence of bridges similar to those generated in Tc–S^0 medium (Fig. 12a). (**c**) Tc–S^0+hematite medium after cocultivation. (**d**) Tc+hematite medium in which *T. globiformans* was monocultivated. (**e**) Tc+hematite medium in which *M. jannaschii* was monocultivated. (**f**) Tc+hematite medium supplemented with 40 mM Na_2S (pH 7.0) and abiotically incubated at 68°C for 16 h. Bar = 1 μm.

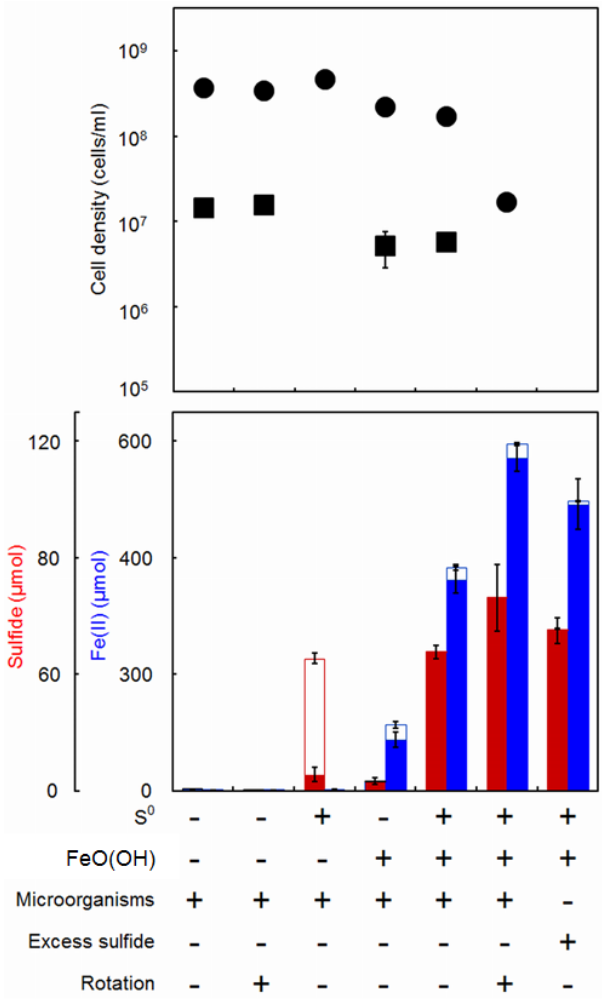

Fig. 18. Reduction of S^0 and FeO(OH) by cocultivation or incubation.

Cocultivation was performed under the conditions shown in the table below the lower graph. Cell densities of *T. globiformans* (circles) and *M. jannaschii* (squares) are plotted in the upper graph, while sulfide and Fe(II) are shown in the lower graph, in which the open and closed red bars indicate soluble and solid sulfides, respectively, and the open and solid blue bars indicate soluble and solid Fe(II), respectively. When the standard deviations are too small, the error bars are hidden by symbols.

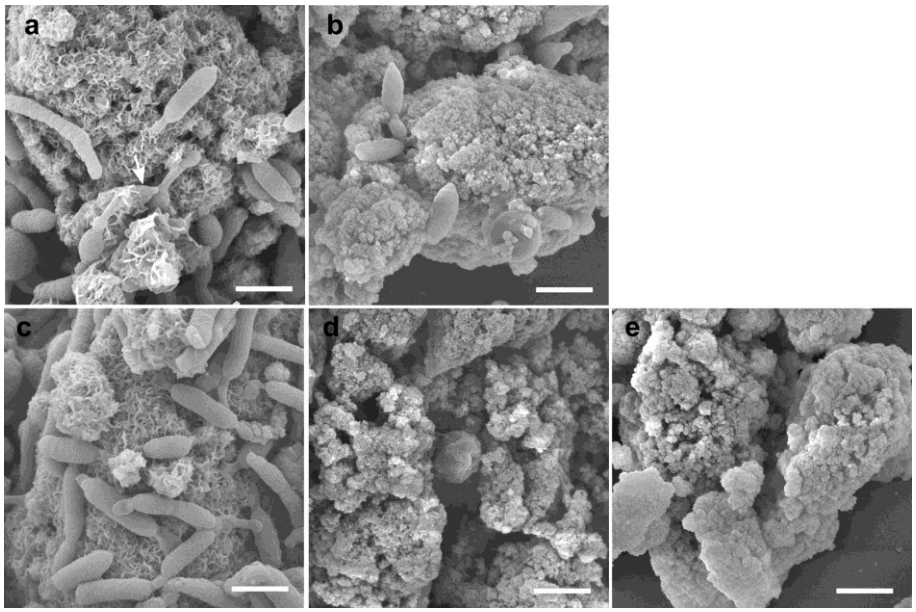

Fig. 19. FE-SEM images of the sediments of Fe(III) oxyhydroxide-containing media.

(**a**) Tc+FeO(OH) medium after cocultivation (**b**) Tc–S^0+FeO(OH) medium after cocultivation. (**c**) Tc+FeO(OH) medium in which *T. globiformans* was monocultivated. (**d**) Tc+FeO(OH) medium in which *M. jannaschii* was monocultivated. (**e**) Tc+FeO(OH) medium supplemented with 40 mM Na_2S (pH 7.0) and abiotically incubated at 68°C for 16 h. *Arrow*, *T. globiformans* rod modestly covered with spiny structures. Bar = 1 μm.

Acknowledgements

I would like to express my deepest gratitude to my supervisor, Prof. Dr. Tomohiko Kuwabara, University of Tsukuba, for his valuable advice and continuous encouragement throughout my research.

My sincere appreciation is extended to Prof. Dr. Kunio Yamane, Prof. Dr. Yoshihiro Shiraiwa, Prof. Dr. Iwane Suzuki and Prof. Dr. Shinichi Miyamura, University of Tsukuba, for their advice during my research.

Gratitude also goes to Prof. Dr. Yasuhisa Yamamura, University of Tsukuba, for his kind help with XRD analysis.

I am also grateful to Prof. Dr. Motoo Utsumi, University of Tsukuba, for his great help with quantification of methane.

I have to express my gratitude to Prof. Dr. Urumu Tsunogai, Nagoya University, for quantification of hydrogen.

Special thanks must go to Dr. Haruyo Yamaguchi, National Institute for Environmental Studies, for her help with electron microscopy.

Finally, I would also like to extend my deepest gratitude to my parents for their continuous support and encouragement during my research.